Research Square

Preprints are preliminary reports that have not undergone peer review.
They should not be considered conclusive, used to inform clinical practice,
or referenced by the media as validated information.

Seismic amplitude of the reservoir-top reflection indicates gas flow where logs and core do not: calibrating 3D seismic attributes against drill-stem tests in a tight fractured quartzite, Attahaddy Field, Sirte Basin, Libya

Gheith Alfakri

Ghate_emg@yahoo.com

Sirte Oil Company

Research Article

Keywords: seismic amplitude, top reflection, drill-stem test, fractured reservoir, tight gas, quartzite, unconformity, Sirte Basin, Libya

Posted Date: November 13th, 2026

DOI: https://doi.org/10.21203/rs.3.rs-11511991/v1

License: This work is licensed under a Creative Commons Attribution 4.0 International License.
Read Full License

Additional Declarations: No competing interests reported.

Seismic amplitude of the reservoir-top reflection indicates gas flow where logs and core do not: calibrating 3D seismic attributes against drill-stem tests in a tight fractured quartzite, Attahaddy Field, Sirte Basin, Libya

Gheith Alfakri

Exploration Department, Sirte Oil Company, Marsa El Brega, Libya

Corresponding author: Ghate_emg@yahoo.com

Abstract

In the Cambro-Ordovician Gargaf quartzite of the Attahaddy gas field, Sirte Basin, Libya, porosity is about 3%, most core plugs have no measurable permeability, and neither logs nor core predict which drill-stem tests (DSTs) flow gas. We test whether 3D seismic amplitude does, computing all attributes directly from the SEG-Y volume. The DST labels were first audited against the written test results: field-wide, four tests recorded as tight had flowed gas through a choke and three were invalid because the packer failed. Over the corrected set of 59 gas-flowing or tight Gargaf DSTs in 27 wells, the average positive peak value in the 0–20 ms window below the Gargaf pick, chosen before the labels were corrected, is higher at gas-flowing tests (median 3,276 against 1,890; $p = 0.004$) and raises the leave-one-well-out AUC of a model of test depth and interval length from 0.825 to 0.874 (permutation $p = 0.034$), although the bootstrap interval of this gain includes zero. A scan of 78 windows locates the signal in the top-reflection complex: every window that improves the model by 0.05 or more overlaps it, while windows in the overburden or more than 40 ms inside the quartzite add no predictive value. The window spanning the whole complex, from 20 ms above to 40 ms below the pick, raises the AUC to 0.992 (0.98–0.99 when whole areas of the field are left out), and remains significant when the window search is repeated inside every permutation ($p = 0.035$). Gas-flowing intervals extend deeper where this reflection is bright. Neither the fluid nor the borehole-scale impedance contrast explains the amplitude, and a fracture-spacing model fitted to the same DSTs gives conductive fractures about 120 ft apart along the hole where the top reflection is bright and about 430 ft where it is dim ($p = 0.003$). We interpret the amplitude as a seismic-scale proxy for open-fracture density below the unconformity. Only three of the 27 wells never flowed gas, so the well-level evidence is weak and confirmation in more wells is needed; within that limit, the top reflection is the first measurement in this field that adds information on flow beyond structural position.

Keywords: seismic amplitude; top reflection; drill-stem test; fractured reservoir; tight gas; quartzite; unconformity; Sirte Basin; Libya

Introduction

In tight fractured reservoirs, wells produce from a small number of conductive fractures, and the matrix contributes little directly (Nelson, 2001). Where those fractures are cannot be predicted reliably from wells alone. The Gargaf quartzite of the Attahaddy gas field, Sirte Basin, Libya (Hallett, 2002; Hallett and Clark-Lowes, 2016), is an extreme case. Core plugs from intervals that flowed gas at several million cubic feet per day have the same near-zero porosity and permeability as plugs from intervals that were tight. Log attributes add little to structural position and tested-interval length in predicting which drill-stem tests (DSTs) flow (Alfakri, unpublished a, c), and water reaches the wells through the same fractures, unseen by the logs (Alfakri, unpublished a, b).

Seismic data sample the rock between wells and over volumes far larger than a borehole, so they may record fractured rock that wells miss. Amplitude, frequency, coherence and attenuation attributes are widely used to map faults, fractures and reservoir quality (Taner et al., 1979; Hart, 1999; Chopra and Marfurt, 2007; Barnes, 2016). With few wells and many candidate attributes, however, correlations arise by chance (Kalkomey, 1997; Hampson et al., 2001). Two further risks are less often discussed. Horizon-based attributes depend on the window, the reference event and snapping options, so a window can move from the reservoir into the overburden without the user noticing. And the well outcomes against which attributes are calibrated are themselves interpretations of old test reports.

This paper addresses all three risks. Working from the SEG-Y volume, with DST labels audited against the original records, it asks:

1. Does seismic amplitude differ between Gargaf DSTs that flowed gas and those that were tight, and does it add to depth and interval length under tests designed to expose chance correlations?
2. Which part of the seismic response carries the signal: the overburden, the reflection at the top of the reservoir, or reflections within it?
3. What does the amplitude record: fluid, the borehole-scale contrast at the Gargaf top, or something seen only at seismic scale, such as fracture density?

Geological setting and data

The Attahaddy Field lies at the northern end of the Zelten Platform in the central Sirte Basin (Hallett, 2002; Hallett and Clark-Lowes, 2016). The structure is a NW–SE, asymmetric, faulted anticline about 25 km long, bounded to the SW by the Attahaddy Fault, with throw reaching about 1,950 ft at the Gargaf level (PHH Petroleum Consultants, 2001; Alfakri, 2018). The Gargaf Formation is a hard, brittle orthoquartzite cemented by syntaxial quartz overgrowths (Tawadros et al., 2001). It is overlain unconformably by Upper Cretaceous rocks: Maragh shale and sandstone over most of the field, and Kalash limestone directly on the Gargaf where the Maragh is absent on the crest (Shaladi, 1990; PHH Petroleum Consultants, 2001). Gas is held in a fracture network; matrix porosity averages about 3% and most plugs have no measurable permeability (Alfakri, unpublished a, c).

A 3D survey was acquired in 2013 and the Gargaf top was interpreted in two-way time (Alfakri, 2018). For this study, a sub-volume of the full-stack, pre-stack time-migrated (PSTM) data was exported as SEG-Y: 302 inlines by 401 crosslines (inlines 1900–2201, crosslines 6245–6645) at 25 m bin spacing, about 76 km², with 4 ms sampling. The inline–crossline grid was tied to UTM zone 34N coordinates by an affine transform fitted to four points from the interpretation project (residuals ≤ 12 m). The interpreted Gargaf time surface (Fig. 1a) was sampled at every trace. Polarity follows the volume as delivered. In the field-wide average aligned on the horizon, a trough about 20 ms above the pick and a peak about 28 ms below it bracket a weak peak at the pick itself (Fig. 2b).

DST labels

Tests outside the Gargaf, misruns, doubtful water recoveries and four tests whose intervals lie above the Gargaf top were removed (Alfakri, unpublished a). Tests had been labelled gas-flowing when the summary gave a gas rate, and tight otherwise. Because this rule depends on whether a rate was written down, the written results of all 31 Gargaf tests labelled tight in the field were re-read. Four had flowed gas through a choke at measurable wellhead pressure and were relabelled gas-flowing (FF4 DST-2, 450–280 psi on a ¾-in. choke; FF15 DST-1, up to 800 psi on ¾ in.; FF31 DST-1, up to 368 psi on ½ in.; FF44

DST-1, 130 psi on ½ in. after 32 hours). Three were removed because the packer failed (FF8 DST-2, FF9 DST-3, FF14 DST-1). Tests that brought only small or late gas to surface, or none, remain tight; only five of the 31 showed no flow at all (Alfakri, unpublished d). Inside the seismic sub-volume, three tests were relabelled (FF4, FF31 and FF44) and one was removed (FF8); FF15, FF9 and FF14 lie outside it.

Twenty-seven wells with valid Gargaf tests lie inside the sub-volume, with 42 gas-flowing and 17 tight tests. Twenty-four wells have at least one gas-flowing test and three have only tight tests (FF12, FF13 and FF18). Three tests recovered formation water (two in FF7, one in FF13) (Fig. 1a). Deviation surveys in the well files examined (FF11, FF12) show drift of 2° or less to total depth, and wells were treated as vertical. Sonic logs across the Gargaf top exist in 24 of the 27 wells and usable density logs in 17.

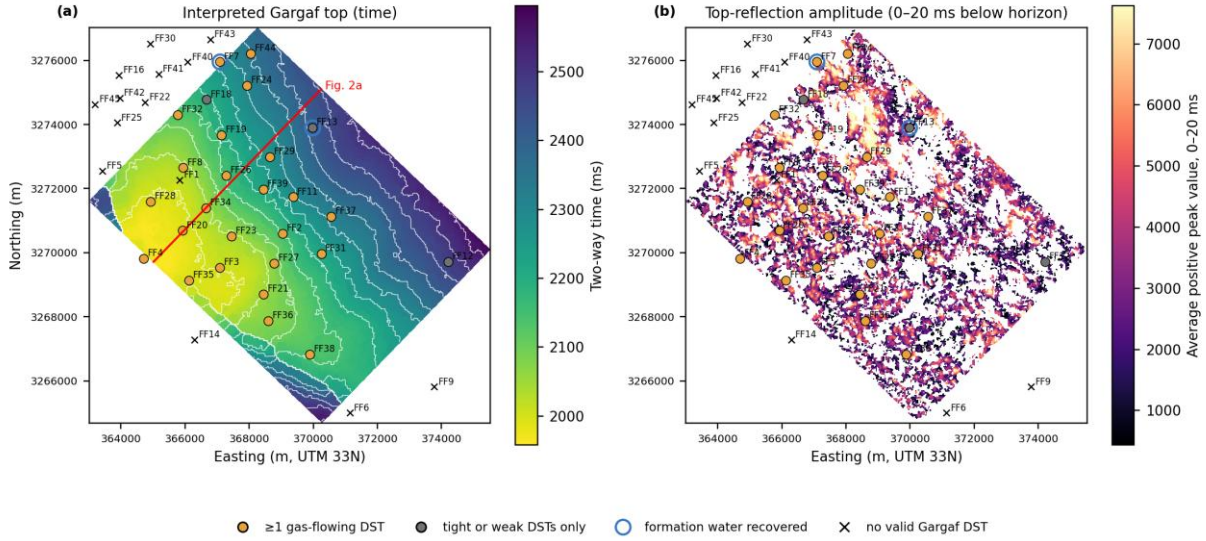


Fig. 1. (a) Interpreted Gargaf top in two-way time within the SEG-Y sub-volume (contours every 50 ms), with wells coloured by their Gargaf DST results (corrected labels): orange, at least one gas-flowing test; grey, only tight tests; blue ring, formation water recovered; crosses, no valid Gargaf DST. The red line is the section in Fig. 2a. (b) Average positive peak value in the 0–20 ms window below the horizon. White: no positive peak inside the window on that trace.

Methods

Attribute extraction

For each trace, the average positive peak value was computed in a window defined relative to the Gargaf pick: the mean of all local maxima with positive amplitude inside the window (Barnes, 2016). Root-mean-square (RMS) amplitude was computed in the same windows. The main attribute is the 0–20 ms window below the pick, which samples the upper part of the top-reflection complex (Fig. 1b). It was chosen in an earlier analysis of the same tests with uncorrected labels and kept unchanged here. Comparison windows were 100–0 ms, 60–0 ms and 100–20 ms above the pick (overburden), 0–100 ms below (top reflection plus upper reservoir), and 20–120 ms and 20–220 ms below (reservoir interior). To locate the signal without choosing windows in advance, all 78 windows with start and end between 120 ms above and 120 ms below the pick were scanned in 20 ms steps. At each well, an attribute is the median over the traces within a 300 × 300 m square centred on the wellhead (typically 144 traces; only 12 and 18 for FF4 and FF7, at the edge of the sub-volume).

Statistical tests

Gas-flowing and tight tests were compared with the Mann–Whitney test. All tests in a well share one seismic value, so test-level p-values are optimistic; the comparison was therefore repeated at well level (wells with at least one gas-flowing test against tight-only wells). Predictive value was assessed relative to the two quantities that already explain much of the DST outcome (Alfakri, unpublished a): subsea mid-depth of the tested interval and the logarithm of interval length. Logistic models (Hosmer et al., 2013) with and without the attribute were scored by the area under the ROC curve (AUC) (Fawcett, 2006) out of sample, by leave-one-well-out (LOWO) prediction and by spatial-block prediction with 4, 6 or 8 areas defined by k-means clustering of well coordinates (Roberts et al., 2017). Models were fitted with scikit-learn (Pedregosa et al., 2011).

To test whether a gain in AUC could arise by chance, the attribute values were reassigned at random between wells (keeping the tests of a well together) 1,000 times and the LOWO gain recomputed (Good, 2005); the p-value is (number of reassignments with a gain at least as large as observed + 1)/1,001. Because the window scan selects the best of 78 windows, its result was tested with a max-statistic permutation test (Westfall and Young, 1993): in each of 200 reassignments the whole scan was repeated and the largest gain kept. A 95% interval for the gain was obtained by resampling wells with replacement 300 times (Efron and Tibshirani, 1993). Structural position (horizon time) and the unit overlying the Gargaf (Maragh or Kalash) were tested as confounders.

Reflection events, rock physics and well ties

Each trace within 150 m of a well was aligned on the horizon, and the amplitudes of five events in the field-average waveform were measured: the peak about 44 ms above the pick (P−44), the trough about 20 ms above (T−20), the peak at the pick (P0), the peak about 28 ms below (P+28) and the trough about 52 ms below (T+52). These were defined after inspecting the data and are treated as exploratory. At wells with sonic coverage across the Gargaf top, the P-velocity contrast was computed from the medians of the logs 5–60 ft above and below it, and the impedance contrast where usable density was available (2.2–2.9 g/cm³, density correction below 0.08 g/cm³, hole in gauge). Synthetic seismograms with Ricker wavelets of 20, 25 and 30 Hz were compared with the median seismic trace within 50 m of the well, allowing a bulk shift of up to ±32 ms (White, 1980).

Spacing of flowing fractures

If conductive fractures are spaced randomly along the hole with mean spacing s, a tested interval of length L intersects at least one with probability $1 - \exp(-L/s)$, and a test is expected to flow when it does (Alfakri, unpublished a). The spacing was estimated by maximum likelihood from the outcomes and lengths of the tests, separately for wells with top-reflection amplitude above and below the well median, with 95% profile-likelihood intervals and a likelihood-ratio test for a common spacing.

Results

The top reflection and the reservoir interior

Above the Gargaf, the Upper Cretaceous and Tertiary section is imaged as continuous, parallel reflections (Fig. 2a). The Gargaf top is the base of this layered package and is marked by a trough–peak pair whose strength varies along the horizon. Below it, the quartzite is imaged as short, discontinuous events. Semblance coherence (Marfurt et al., 1998) is uniformly low below the horizon, and low-coherence zones in the overburden do not form chimneys or pipes rising from the Gargaf. The strongest, most coherent information about the quartzite is therefore the reflection at its top.

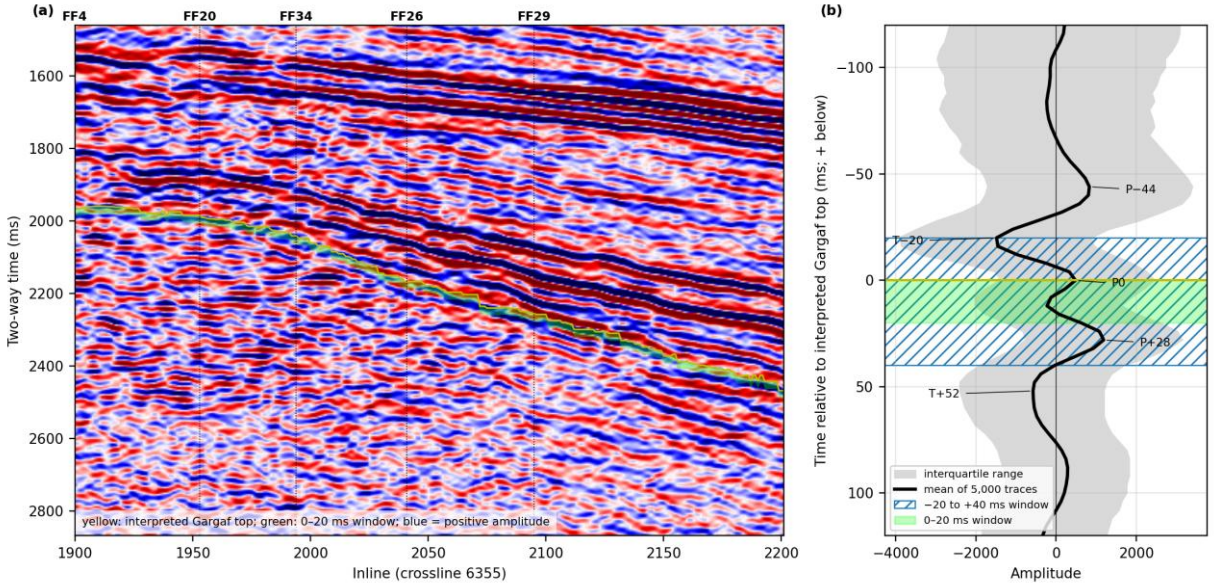


Fig. 2. (a) Seismic section through FF4, FF20, FF34, FF26 and FF29 (location in Fig. 1a). Yellow: interpreted Gargaf top; green: 0–20 ms window below it. (b) Mean (black) and interquartile range (grey) of 5,000 traces aligned on the horizon, with the reflection events, the 0–20 ms window (green) and the −20 to +40 ms window spanning the top-reflection complex (hatched).

Where the signal lies

Depth and interval length alone give a LOWO AUC of 0.825 for the 59 gas-flowing and tight tests (Table 1). Adding the 0–20 ms amplitude raises it to 0.874 (gain 0.049; permutation p = 0.034), and to 0.884–0.895 when whole areas are left out (against 0.808–0.817 without it). Windows that exclude the top reflection add no predictive value (Fig. 3b): 20–120 ms below gives 0.803 (p = 0.46), 20–220 ms gives 0.829 (p = 0.17), and the three overburden windows give 0.723–0.783 (p = 0.76–0.98). The 0–100 ms window, which contains the top reflection diluted by the interior, gives 0.831 (p = 0.12).

The window scan (Fig. 3a) shows the same pattern without pre-selected windows. Five of the 78 windows raise the AUC by 0.05 or more, and all five overlap the top-reflection complex. No window starting 40 ms or more below the pick adds more than 0.013, and the median gain of windows lying wholly in the overburden is −0.05. The best window spans the whole complex, from 20 ms above to 40 ms below the pick, and raises the AUC from 0.825 to 0.992. Because it was found by searching, its significance was assessed with the search repeated in every permutation: only 6 of 200 reassignments produced a best window with a gain at least as large (p = 0.035; Fig. 4c). The narrower 0–20 ms window, by contrast, is not distinguishable from the best window found by chance (p = 0.52 in the same test), although it is significant when tested as a single window. Its bootstrap interval of gain also includes zero (−0.04 to 0.34).

Table 1. Amplitude by DST outcome and added predictive value, by window (average positive peak value; 59 tests in 27 wells, corrected labels). Medians over gas-flowing and tight tests, with Mann–Whitney p (tests treated as independent). LOWO AUC with depth, interval length and the attribute (base 0.825). Permutation p from 1,000 random reassignments between wells (200 for 60–0 ms, 100–20 ms, 20–220 ms and RMS); for the −20 to +40 ms window, which was selected by the scan, p is adjusted for the search over 78 windows.

Window (relative to Gargaf pick)	Gas / tight median (p)	LOWO AUC	Gain	Permutation p
100–0 ms above	4,331 / 4,829 (0.15)	0.723	−0.102	0.98
60–0 ms above	4,598 / 4,598 (0.91)	0.783	−0.042	0.76
100–20 ms above	4,520 / 4,829 (0.17)	0.742	−0.083	0.97

Window (relative to Gargaf pick)	Gas / tight median (p)	LOWO AUC	Gain	Permutation p
0–20 ms below (fixed in advance)	3,276 / 1,890 (0.004)	0.874	+0.049	0.034
20 ms above to 40 ms below (whole complex)	3,764 / 3,008 (0.030)	0.992	+0.167	0.035 (search-adjusted)
0–100 ms below	3,087 / 3,087 (0.76)	0.831	+0.006	0.12
20–120 ms below	3,000 / 3,412 (0.96)	0.803	−0.022	0.46
20–220 ms below	2,808 / 2,887 (0.056)	0.829	+0.004	0.17
RMS, 0–20 ms below	2,423 / 2,204 (0.017)	0.856	+0.031	0.065

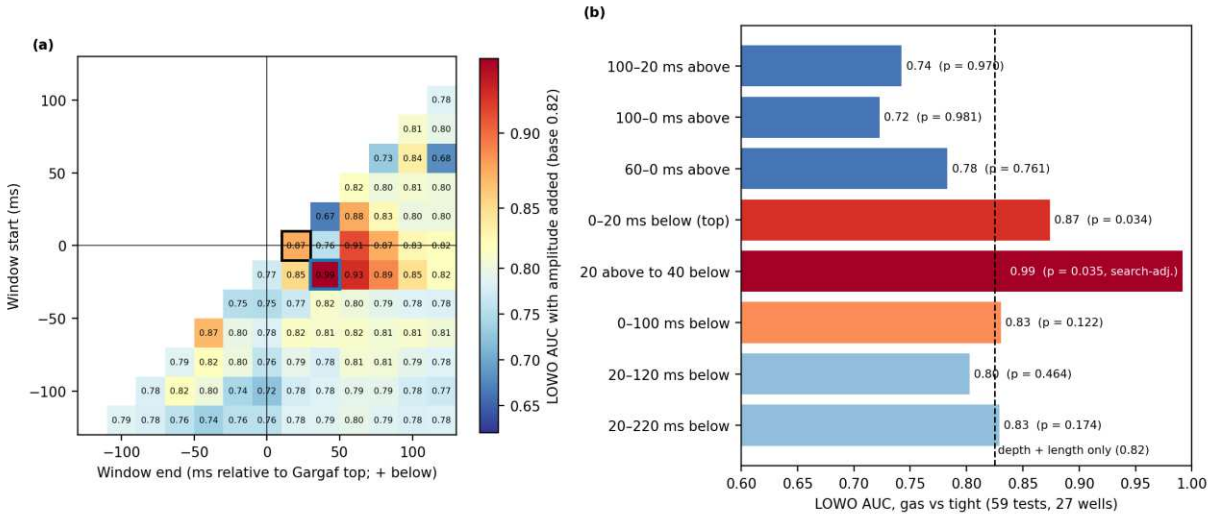


Fig. 3. (a) LOWO AUC of the model with depth, interval length and average positive peak value, for every window with start and end between 120 ms above and 120 ms below the Gargaf pick (20 ms steps; negative = above). Black square: the 0–20 ms window fixed in advance; blue square: the −20 to +40 ms window. (b) LOWO AUC for the windows of Table 1, with permutation p-values; the dashed line is the base model.

The top-reflection amplitude and DST outcome

Gas-flowing tests lie on stronger top-reflection amplitude than tight tests (Fig. 4a). Over the whole complex, the proportion of gas-flowing tests rises from 52% in the lowest tercile of amplitude to 74% in the middle and 93% in the highest (Fig. 4b); for the 0–20 ms window the figures are 48%, 75% and 94%. The gain of the whole-complex window persists when whole areas are left out (AUC 0.980, 0.992 and 0.989 for 4, 6 and 8 areas, against 0.808–0.817), its bootstrap interval excludes zero (0.005–0.38), and it stays positive (0.06–0.23) whichever single well is left out. The combination of amplitude and depth separates the tests because the depth below which tests are tight increases with amplitude (Fig. 5): in the fitted model the 50% boundary deepens by roughly 600–700 ft for every 1,000-unit increase in amplitude (the model nearly separates the two classes, so the slope is poorly constrained). Where the top reflection is dim, gas-flowing tests are confined to the upper Gargaf; where it is bright, gas flowed from below −11,500 ft subsea (FF7, and the relabelled FF44 DST-1).

At well level the evidence is weak. The three tight-only wells have lower amplitude than the 24 wells with gas-flowing tests (median 3,008 against 3,606 for the whole complex; 2,520 against 3,276 for 0–20 ms), but the difference is not significant ($p = 0.12$ and 0.23). Among gas-flowing tests, amplitude does not correlate significantly with the reported gas rate ($\rho = 0.25$, $p = 0.15$, 34 tests). The tests of the tight-only wells FF12 and FF13 are also the deepest in the data set (mid-depths about −12,140 to −12,230 ft subsea),

close to the gas–water contact, and FF13 recovered formation water, so the well-level comparison partly reflects position in the column.

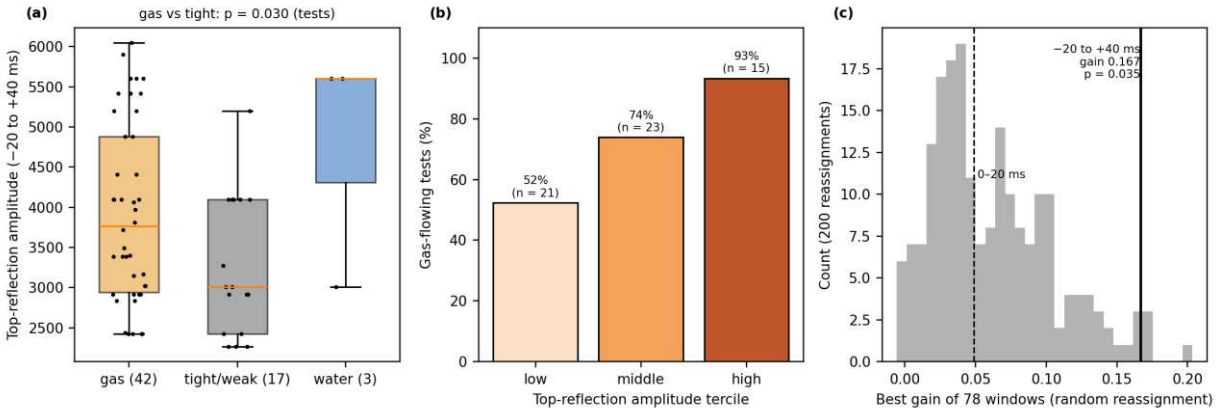


Fig. 4. (a) Top-reflection amplitude (−20 to +40 ms) at the wells for gas-flowing, tight and formation-water DSTs (number of tests in brackets); p: Mann–Whitney test of gas-flowing against tight tests, treating tests as independent. (b) Share of gas-flowing tests in each tercile of amplitude. (c) Best gain in LOWO AUC over the 78-window scan after 200 random reassignments of amplitude between wells (grey), with the observed gains of the −20 to +40 ms window (solid) and the 0–20 ms window (dashed).

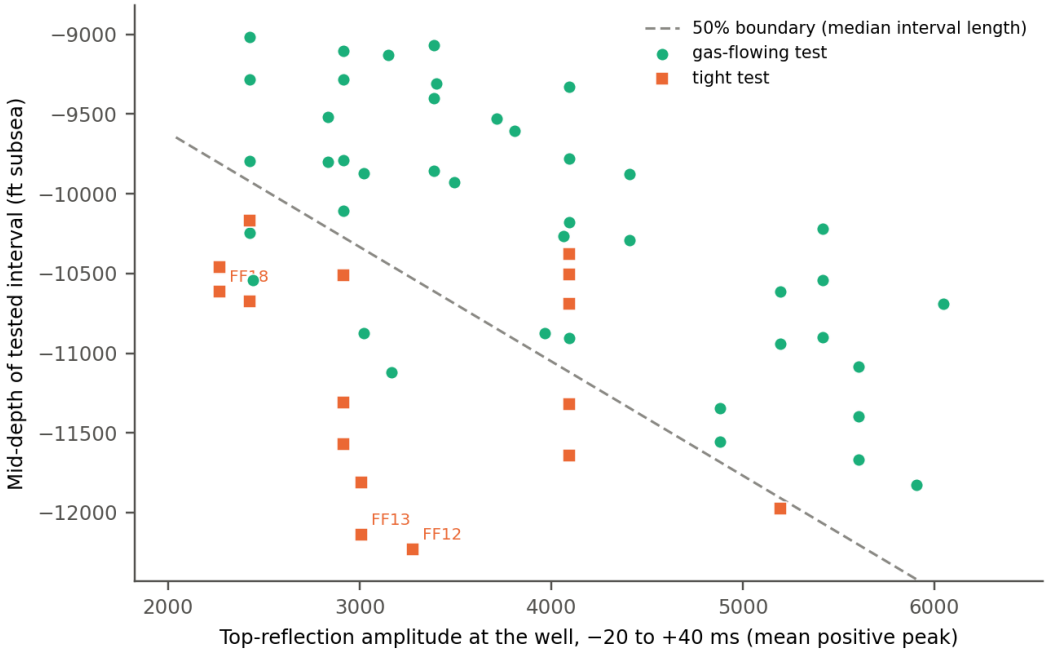


Fig. 5. Mid-depth of each tested interval against the top-reflection amplitude at the well (−20 to +40 ms), for gas-flowing (green) and tight (orange) tests. Dashed line: 50% boundary of the logistic model at the median interval length. Labelled points: the deepest tests of the three tight-only wells.

Neither of the two obvious confounders explains the result. Adding horizon time to the model gives 0.863 with the 0–20 ms amplitude and 0.987 with the whole-complex amplitude, against 0.811 without either. Amplitude is stronger where Maragh overlies the Gargaf (0–20 ms median 3,276) than where Kalash limestone does (1,764), but gas-flowing tests lie on stronger 0–20 ms amplitude within both groups (Maragh: 35 tests in 19 wells, p = 0.009; Kalash: 24 tests in 8 wells, p = 0.019). For the whole-complex window the difference is significant under Maragh (p = 0.003) but not under Kalash (p = 0.31). All three tight-only wells are under Maragh, so unit and outcome overlap. Adding the overlying unit to the model gives 0.922 and 0.973 for the two windows, against 0.790 without amplitude.

The event analysis is less clear-cut. Added to depth and length, the trough-to-peak swing T−20 to P+28 gives a LOWO AUC of 0.895 and the trough T−20 0.863, but the peak P+28 alone gives 0.678 and the peak at the pick 0.818, although the latter differs between gas-flowing and tight tests ($p = 0.007$). The overburden peak P−44 gives 0.807 and does not differ between them ($p = 0.61$); the deeper trough T+52 gives 0.807. Gas-flowing tests also show a shorter time from the pick to P+28 (median 28 against 36 ms, two samples; $p = 0.021$, tests treated as independent), which may indicate a thinner or sharper transition at the top. These results were not permutation-tested and are exploratory.

Rock physics and well ties

At the borehole scale, the Gargaf top is a modest increase in impedance: the median velocity contrast is about 0.04 and the median impedance contrast about 0.05. Neither correlates with the seismic amplitude of the top reflection (trough-to-peak swing against velocity contrast, $\rho = 0.26$, $p = 0.21$, 25 wells with sonic logs inside the sub-volume; 0–20 ms amplitude against impedance contrast, $\rho = -0.06$, $p = 0.82$, 17 wells; Fig. 6a). Over all wells with logs in the field, neither differs detectably between wells with gas-flowing tests and tight-only wells (velocity, 27 against 3 wells, $p = 0.95$; impedance, 21 against 2 wells, $p = 0.39$; Fig. 6b), which is weak evidence with so few tight-only wells. Synthetic seismograms tie the seismic only moderately (median best correlation 0.40 over 20 wells; best 0.59 at FF21; Fig. 6c), and the correlation between synthetic and seismic top-reflection amplitude across wells depends on the wavelet and alignment (ρ from −0.56 to 0.47). The log-derived synthetics therefore do not reproduce the lateral variation of the top reflection in any reliable way.

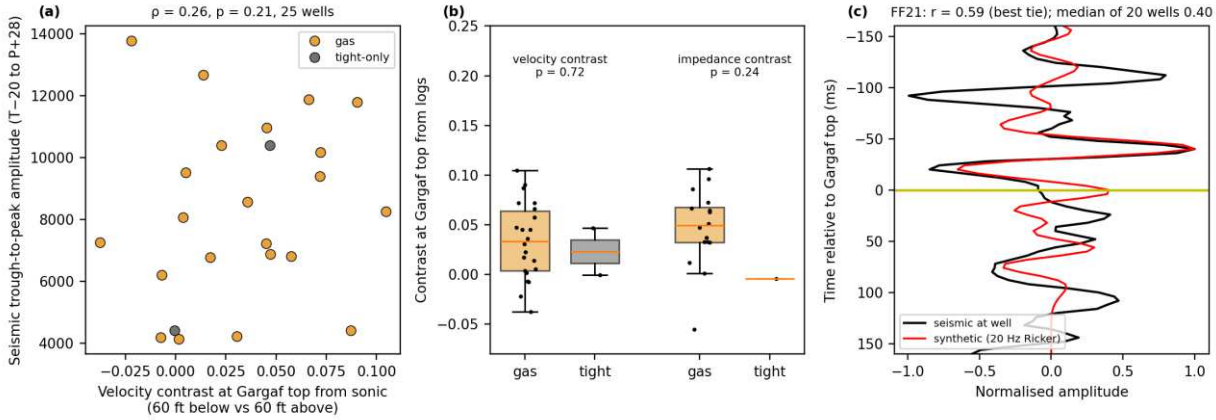


Fig. 6. (a) Seismic trough-to-peak amplitude of the top reflection (T−20 to P+28) against the P-velocity contrast at the Gargaf top from the sonic log. (b) Velocity and impedance contrasts at the Gargaf top in wells with gas-flowing tests and tight-only wells. (c) Synthetic seismogram (red; 20 Hz Ricker) against the seismic trace at the well (black) for FF21, the best tie.

Spacing of flowing fractures

Fitted to all 59 tests, the random-fracture model gives a mean spacing of conductive fractures of 295 ft along the hole (95% interval 209–428 ft). In wells where the 0–20 ms amplitude is at or above the well median (3,213; 25 tests in 14 wells), the spacing is 120 ft (55–246 ft); in wells below it (34 tests in 13 wells), 433 ft (272–734 ft) (Fig. 7a, b). A common spacing is rejected (likelihood-ratio $p = 0.003$, treating tests as independent). Splitting the wells by the whole-complex amplitude instead gives 193 ft (115–332 ft) against 416 ft (254–723 ft) ($p = 0.041$). In bright areas, a 300 ft test, close to the median length, has a modelled 92% chance of intersecting a conductive fracture; in dim areas, 50%.

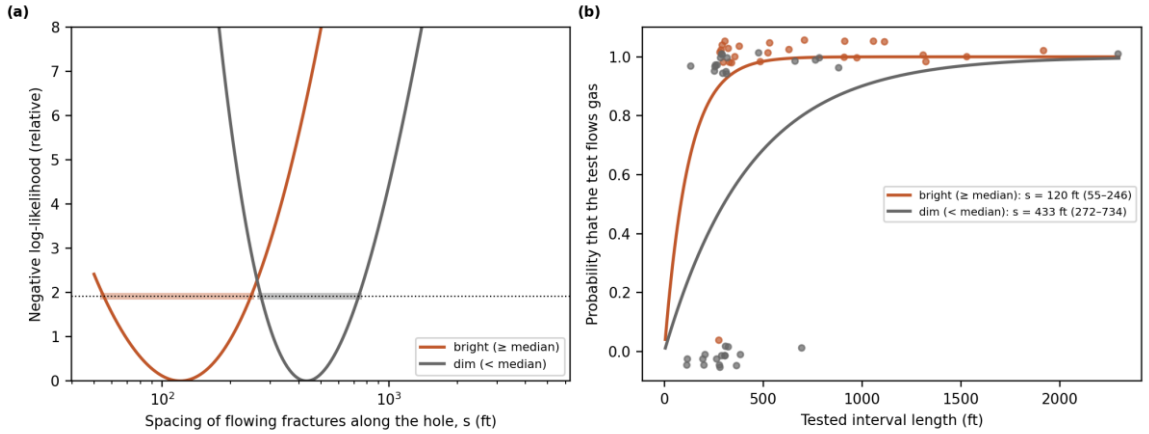


Fig. 7. (a) Negative log-likelihood of the mean spacing of conductive fractures for tests in wells with bright (orange) and dim (grey) top reflection (0–20 ms, split at the well median); shaded: 95% intervals. (b) Modelled probability that a test flows gas against tested-interval length, with the observed outcomes (1 = gas-flowing, 0 = tight; jittered).

Discussion

Why the top reflection

In the Gargaf, the seismic contains little organised energy below the top: the quartzite is massive, its internal contrasts are weak or below seismic resolution (Widess, 1973), and the image is degraded by depth, fault shadows and multiples from the layered overburden. Windows within the reservoir therefore add no predictive value (Table 1). The reflection at the top is the strongest and most continuous event at reservoir level; it integrates the elastic properties of the uppermost tens of metres of the quartzite over a Fresnel zone of several hundred metres. If any seismic property of the reservoir relates to flow, it is most likely to be seen there, and that is what the window scan shows. That the best window spans the whole trough–peak complex, rather than one lobe of it, suggests that the signal is the strength of the complex as a whole.

What the top-reflection amplitude records

The amplitude is not a fluid indicator. At 3% porosity, rock physics calibrated to the field sonic predicts a negligible impedance difference between gas- and water-bearing quartzite (Alfakri, unpublished c), and the two formation-water tests in FF7 lie on some of the strongest amplitudes in the field (Fig. 4a), whereas the water test in FF13 lies on low amplitude. Nor does it follow the borehole-scale contrast at the unconformity, and although it is stronger under Maragh than under Kalash, neither the overlying unit nor structural position explains its association with flow. What remains is a property of the uppermost quartzite that the seismic sees and a borehole does not. Seismic amplitude at a boundary depends not only on the contrast measured in one hole but on its lateral continuity and sharpness over the Fresnel zone, and on interference within the transition (Widess, 1973; Hilterman, 2001). A zone of open fractures, brecciation or dissolution below the unconformity changes all three, and can be thin or absent at a wellbore while well developed around it. The fracture-spacing model, fitted to the same tests, expresses the amplitude–outcome association as a fracture density: where the top reflection is bright, conductive fractures are two to four times more closely spaced along the hole. Fracture spacing is the quantity that controls whether a DST flows (Alfakri, unpublished a), and it is independent of the fluid, consistent with water-bearing FF7 also being bright. It is a re-expression of the association rather than independent evidence. The deeper reach of gas-flowing intervals in bright wells (Fig. 5) fits the same picture. We

therefore interpret the top-reflection amplitude as a proxy for the density of open fractures in the upper part of the reservoir.

This interpretation can be tested. Image logs should show closer fracture spacing in the upper Gargaf of bright wells, and pre-stack data should show azimuthal anisotropy or AVO behaviour consistent with aligned fractures (Avseth et al., 2005).

Lessons for attribute calibration

Three steps changed the evidence in this study by as much as the effect itself. First, an earlier analysis used horizon-attribute maps exported from the interpretation project; recomputing them from the SEG-Y showed that two of them sampled windows lying largely above the horizon rather than the windows their settings implied, probably because event-snapping options pulled parts of the windows onto the strongest event. A horizon attribute should therefore be verified against the trace data before it is interpreted geologically (Kalkomey, 1997). Second, re-reading the DST reports changed seven of 31 tight labels; with uncorrected labels the 0–20 ms window gave $p = 0.013$ rather than 0.034. Third, a window found by searching must be tested with the search included (Westfall and Young, 1993). A companion study (Alfakri, unpublished d) also tested spectral, inversion, diffraction, coherence and curvature attributes at the same wells: none performed better than the top-reflection amplitude, and if all six attribute families are counted, the evidence for the best window weakens to $p \approx 0.21$. With only three tight-only wells, about 60 wells would be needed for a decisive test (Alfakri, unpublished d).

Use for well placement

In the Gargaf, the top-reflection amplitude is the first measurement that adds to structural position in predicting flow. It can rank locations within a structural level and indicate how deep in the Gargaf a test is likely to flow, and it suggests longer test intervals where the top reflection is dim, because conductive fractures there are more widely spaced. The same workflow applies to other tight fractured reservoirs beneath an unconformity, such as the Cambro-Ordovician quartzites of the Murzuq, Ghadames and Illizi basins: audit the well outcomes; calibrate the attribute against DST or production results; keep only what adds to depth and interval length under out-of-sample and permutation tests; verify the extraction window on the trace data; and include any window search in the significance test. Because water also flows through bright, fractured rock, a bright top reflection near the water level indicates a risk of early water as well as a chance of gas.

Limitations

Twenty-seven wells contribute and only three have only tight tests; all tests in a well share one seismic value. The cross-validation and permutation tests account for this, but the well-level comparison is not significant, and the result should be regarded as evidence from one field that needs confirmation. The event analysis is exploratory. The labels remain a judgement: tests with small or late gas were kept as tight. The attribute is a median over 300 × 300 m around vertical wellheads (fewer traces at FF4 and FF7), whereas DST intervals sample a few hundred feet of the hole. The sub-volume covers 27 of the wells with valid tests, and the georeferencing relies on four tie points. Well ties are moderate, so the rock-physics conclusions rest on log contrasts rather than on a calibrated wavelet. The fracture-spacing model assumes randomly spaced fractures and that one conductive fracture is enough for a test to flow (Alfakri, unpublished a).

Conclusions

1. In the tight Gargaf quartzite of the Attahaddy Field, where logs and core do not predict flow, DSTs that flowed gas lie on stronger amplitude of the Gargaf top reflection than tight tests.
2. The amplitude in the 0–20 ms window adds to test depth and interval length (LOWO AUC 0.825 to 0.874; permutation p = 0.034). A window spanning the whole top-reflection complex adds much more (AUC 0.992) and remains significant after allowing for the search over 78 windows (p = 0.035).
3. The predictive signal is confined to the top-reflection complex; windows inside the seismically chaotic quartzite and in the overburden add no predictive value.
4. The amplitude does not record the fluid or the borehole-scale impedance contrast. A fracture-spacing model puts conductive fractures about 120 ft apart where it is bright and 430 ft where it is dim, and gas-flowing intervals reach deeper below bright reflections, so it is interpreted as a seismic-scale proxy for open-fracture density below the unconformity.
5. Auditing the DST labels, verifying attribute windows on the trace data and including window searches in significance tests each changed the evidence materially. With only three tight-only wells, confirmation in more wells is needed.

References

Alfakri, G., 2018. Integrated petroleum geosciences study of Attahaddy Gas Field (Sirte Basin, Libya). 3rd World Congress on Petroleum Engineering and Natural Gas Recovery, Sydney. Journal of Petroleum and Environmental Biotechnology (conference abstract). https://doi.org/10.4172/2157-7463-C1-041

Alfakri, G., unpublished a. Fracture-borne water invisible to logs and core: evidence from drill-stem tests in a tight quartzite gas reservoir, Gargaf Formation, Sirte Basin, Libya.

Alfakri, G., unpublished b. The gas–water contact of the Attahaddy Field: evidence from legacy logs, drill-stem tests, drilling records and pressures in a tight fractured quartzite reservoir (Gargaf Formation, Sirte Basin, Libya).

Alfakri, G., unpublished c. When can logs and seismic tell gas from water in tight rock? Porosity limits from rock physics in the Gargaf quartzite, Sirte Basin, Libya.

Alfakri, G., unpublished d. How much can 60 drill-stem tests prove? Label errors, window selection and multiple testing in the seismic-attribute validation of a tight fractured quartzite, Attahaddy Field, Libya.

Avseth, P., Mukerji, T. and Mavko, G., 2005. Quantitative Seismic Interpretation. Cambridge University Press, Cambridge, 359 pp.

Barnes, A.E., 2016. Handbook of Poststack Seismic Attributes. Geophysical References 21. Society of Exploration Geophysicists, Tulsa.

Chopra, S. and Marfurt, K.J., 2007. Seismic Attributes for Prospect Identification and Reservoir Characterization. Geophysical Developments 11. Society of Exploration Geophysicists, Tulsa.

Efron, B. and Tibshirani, R.J., 1993. An Introduction to the Bootstrap. Chapman and Hall, New York.

Fawcett, T., 2006. An introduction to ROC analysis. Pattern Recognition Letters, 27, 861–874.

Good, P., 2005. Permutation, Parametric and Bootstrap Tests of Hypotheses, 3rd edn. Springer, New York.

Hallett, D., 2002. Petroleum Geology of Libya. Elsevier, Amsterdam.

Hallett, D. and Clark-Lowes, D., 2016. Petroleum Geology of Libya, 2nd edn. Elsevier, Amsterdam.

Hampson, D.P., Schuelke, J.S. and Quirein, J.A., 2001. Use of multiattribute transforms to predict log properties from seismic data. Geophysics, 66, 220–236.

Hart, B.S., 1999. Definition of subsurface stratigraphy, structure and rock properties from 3-D seismic data. Earth-Science Reviews, 47, 189–218.

Hilterman, F.J., 2001. Seismic Amplitude Interpretation. Distinguished Instructor Short Course 4. Society of Exploration Geophysicists and European Association of Geoscientists and Engineers, Tulsa.

Hosmer, D.W., Lemeshow, S. and Sturdivant, R.X., 2013. Applied Logistic Regression, 3rd edn. Wiley, Hoboken.

Kalkomey, C.T., 1997. Potential risks when using seismic attributes as predictors of reservoir properties. The Leading Edge, 16, 247–251.

Marfurt, K.J., Kirlin, R.L., Farmer, S.L. and Bahorich, M.S., 1998. 3-D seismic attributes using a semblance-based coherency algorithm. Geophysics, 63, 1150–1165.

Nelson, R.A., 2001. Geologic Analysis of Naturally Fractured Reservoirs, 2nd edn. Gulf Professional Publishing, Boston.

Pedregosa, F., Varoquaux, G., Gramfort, A., Michel, V., Thirion, B., Grisel, O., Blondel, M., Prettenhofer, P., Weiss, R., Dubourg, V., Vanderplas, J., Passos, A., Cournapeau, D., Brucher, M., Perrot, M. and Duchesnay, E., 2011. Scikit-learn: machine learning in Python. Journal of Machine Learning Research, 12, 2825–2830.

PHH Petroleum Consultants Ltd., 2001. Integrated Reservoir Study, Bahi and Gargaf Intervals, Attahaddy Gas Field: Geology Interim Report III. Unpublished report for Sirte Oil Company, Calgary.

Roberts, D.R., Bahn, V., Ciuti, S., Boyce, M.S., Elith, J., Guillera-Arroita, G., Hauenstein, S., Lahoz-Monfort, J.J., Schröder, B., Thuiller, W., Warton, D.I., Wintle, B.A., Hartig, F. and Dormann, C.F., 2017. Cross-validation strategies for data with temporal, spatial, hierarchical, or phylogenetic structure. Ecography, 40, 913–929.

Shaladi, F.A., 1990. Seismic stratigraphy of the Attahady Field, Concession 6, Sirte Basin, Libya. PhD thesis, University of Glasgow.

Taner, M.T., Koehler, F. and Sheriff, R.E., 1979. Complex seismic trace analysis. Geophysics, 44, 1041–1063.

Tawadros, E., Rasul, S.M. and Elzaroug, R., 2001. Petrography and palynology of quartzites in the Sirte Basin, central Libya. Journal of African Earth Sciences, 32, 373–390.

Westfall, P.H. and Young, S.S., 1993. Resampling-Based Multiple Testing: Examples and Methods for p-Value Adjustment. Wiley, New York.

White, R.E., 1980. Partial coherence matching of synthetic seismograms with seismic traces. Geophysical Prospecting, 28, 333–358.

Widess, M.B., 1973. How thin is a thin bed? Geophysics, 38, 1176–1180.